

High-Speed Photographs of Laser-Induced Heating

This Communication presents some high-speed photographs showing the effects of high-energy, focused laser beams striking targets of steel, brass, and aluminum. For the light flux densities used, these photographs seem to support recent speculations¹⁻³ that the absorption of intense laser radiation will heat the material at some depth below the surface to its vaporization temperature before the material at the surface has absorbed its latent heat of vaporization. This is thought to induce a pulse of high pressure in the underlying material and to result in the emission of the vaporized material similar to a chemical explosion.

In Figs. 1(a) and 1(b), we see the laser beam striking a brass target (an automobile key), and the thermal explosion taking place in Fig. 1(c). The time between frames is approximately 125 μsec . The brass therefore absorbs the laser radiation for approximately 200 μsec before the event we will refer to as a thermal explosion. After the explosion, as can be seen in Figs. 1(d) through 1(h), the material is truly a vapor and rapidly disappears. The vapor progresses in the direction of the laser source, resulting in a deposit on the cover glass that protects the lens. Figure 1(i) shows the brass target 4.75 msec (38 frames) after the initiation of the laser pulse in Fig. 1(a). Note the incandescence of the brass surrounding the area where the laser beam was focused. This series of photographs can be used to estimate the temperature and heat-diffusing properties of this material.

Figure 2 shows a strikingly different series of events. In Fig. 2(a), the laser beam strikes a steel target. Approximately 75 μsec later the surface of the steel begins to evaporate. The plume of vapor leaving the surface is shown in Fig. 2(b). The event which we shall describe as a thermal explosion, however, does not take place until approximately 200 μsec after the initiation of the laser radiation. This is shown in Fig. 2(c). The metal leaving the target during this explosion is in both a vapor and a liquid state. This is clearly shown in Fig. 2(e), where the core of the exploding metal is in the vapor state and the metal surrounding the core is in the liquid state. The liquid particles progress towards the laser, coating the cover glass with splotches of steel. This series of photographs seems to indicate that the steel absorbs

the laser radiation up to the time of the thermal explosion (200 μsec) and then the vapor and liquid metal leaving the material absorb or scatter subsequent laser pulses. The explosive shock from the underlying material travels outward, forcing the metal near the surface to escape as a vapor. The recoil⁴ also travels into the interior of the metal to force the molten metal to exit in the liquid state. Figure 2(i) shows the incandescence surrounding the area where the laser beam was focused, 3.9 msec (31 frames) after the start of laser action.

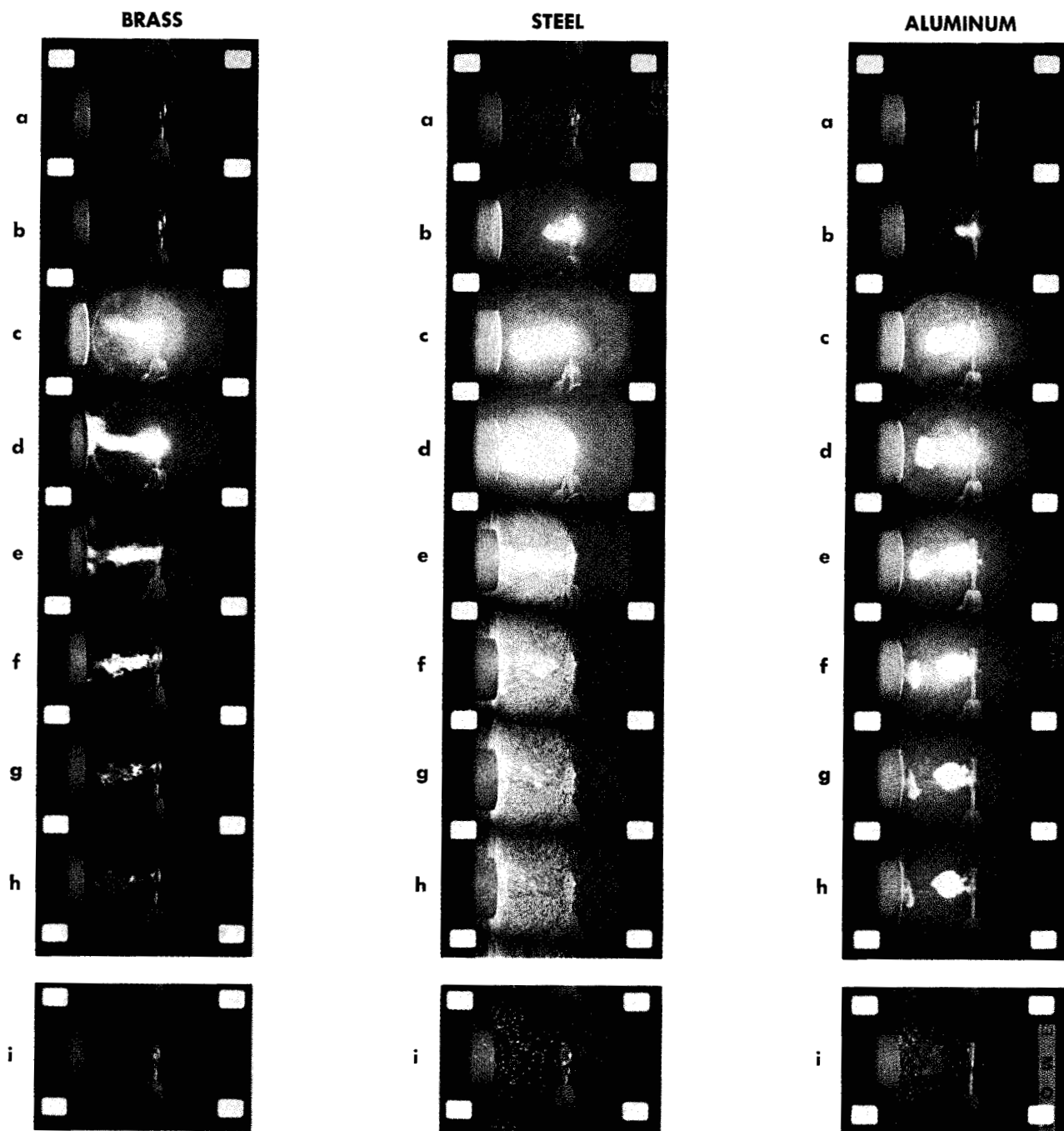
The series of events shown in Fig. 2 seems to have a correlation with the reported^{3,5-7} results of laser-induced emission of electrons and positive ions from metals. In the case of electron current, D. Lichtman and J. F. Ready³ observed strong thermionic emission occurring approximately 50 μsec after the start of lasing action, and decreasing very rapidly after the first 150 μsec . Referring to Fig. 2, we can assume that strong thermionic emission would be initiated some time between Figs. 2(a) and 2(b), or approximately 75 μsec after the start of lasing action. This thermionic emission would continue until some time between Figs. 2(b) and 2(c), just before the thermal explosion. This interval can be estimated to be approximately 200 μsec or less from the start of lasing action. This also agrees with the observations of R. Honig⁵ who reported that with increased laser beam energy the thermionically-induced charged particle spikes formed a continuous pulse which was several hundred microseconds wide but was always extinguished before the end of the laser pulse. Thus there seems to be a strong correlation between the events shown in Figs. 2(a), (b) and (c) and the reported results of laser-induced emission of electrons and positive ions from metals.

Figure 3 shows more dramatically the vapor plume and thermal explosion sequence. In Fig. 3(a), the laser beam is striking an aluminum target. In Fig. 3(b), the surface of the aluminum evaporates, yielding a plume of vapor. The thermal explosion is just beginning to appear in Fig. 3(c). Figure 3(f) clearly shows the second plume of vapor surrounded by molten particles of aluminum. Note in addition the plume of vapor coming off the back surface of the target in Figs. 3(e) and (f). Some molten particles also leave the back surface, as shown in Figs. 3(g) and

Figure 1 High-speed photographs of events taking place when a focused laser beam strikes brass key 0.19 cm thick. The beam is focused on an area of about $7 \times 10^{-3} \text{ cm}^2$. The laser did not penetrate completely through this thickness of brass.

Figure 2 High-speed photographs of the focused laser beam on steel target 0.19 cm thick. The beam is focused on an area of about $7 \times 10^{-3} \text{ cm}^2$. The laser beam did not penetrate completely through the key.

Figure 3 High-speed photographs of the focused laser beam on aluminum target 0.19 cm thick. The beam was focused on an area of about $7 \times 10^{-3} \text{ cm}^2$. The laser beam penetrated completely through in this case. The opening on the surface of the incident laser radiation is 0.8 millimeters in diameter, and the opening on the back surface is 0.4 millimeter in diameter.



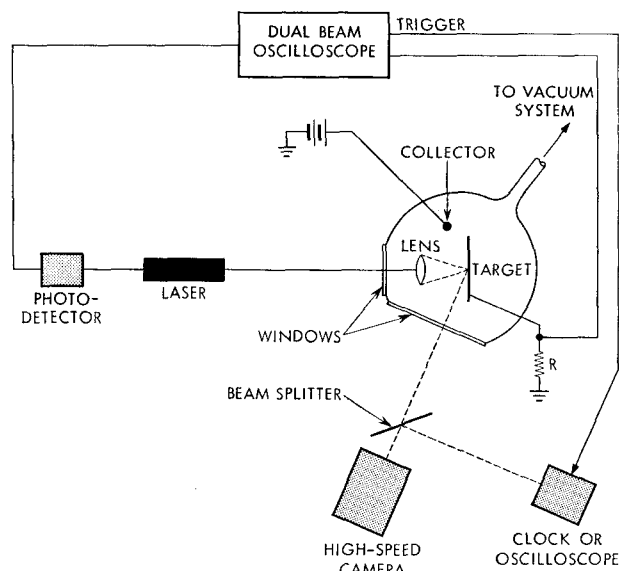


Figure 4 Proposed experimental arrangement for studying the effect of a focused laser beam on specimens.

3(h), but the majority of the material is forced out through the front surface. The incandescence around the area of the incident laser radiation is shown in Fig. 3(i), 2.4 msec (19 frames) after the start of laser action.

The results presented here were obtained with a pulsed ruby laser. The laser crystal used had uncoated ends, and measured 3/8 inches in diameter and 7 inches in length. A properly aligned external dielectric coated mirror tuned for 6943 Å is used at one end of the laser optical cavity. The ruby is located in a cylindrical cavity of elliptical cross section. At the two foci of the ellipse are mounted, respectively, the ruby crystal and a 2000-joule linear xenon flash lamp. The ruby is cooled to 150°K by a stream of cooled nitrogen gas. This laser configuration is capable of yielding a maximum output of approximately 13 joules over an interval of 800 μsec. The beam from the laser is focused by a simple plano-convex lens of 54-mm focal length. The peak power density on the metals was estimated to be about 2×10^6 w/cm². A microscope cover glass placed in front of the lens protected it from the violent reaction of the metals. A Fairchild Motion Analysis high-speed rotating-prism cine camera (Model HS401) was used to record the events which occurred both during and after the incidence of the laser beam on the metal samples. This camera was operated at the rate of 8000 frames per second, with an exposure time of 2.5×10^{-5} seconds per frame. The

camera, equipped with a 3-inch f/1.9 lens, was positioned 24 inches from the object. The film used was Eastman Kodak High Speed Ektachrome (tungsten type), ASA rating 125.

Future experiments to study the heating effects of a focused laser beam should include the simultaneous monitoring of the laser-induced thermionic emission and high-speed photography. The thermionic current gives a good indication of the temperature in the irradiated area, and the photographs would give a visual history of the events which took place during specific intervals of time. These two records would then be studied for correlations. The experimental system shown in Fig. 4 would appear suitable for this purpose. In Fig. 4 the box labeled "clock or oscilloscope" would be triggered at the start of lasing action, and would be optically coupled to the high-speed camera by a beam-splitter arrangement. In this way, time could be recorded simultaneously on the same film with the laser beam-target interaction. Other familiar techniques such as those employed in missile photography can also be used. Color-temperature calibration of the high-speed film would yield a great deal of information concerning the temperature of the target material during and after the laser radiation. Experiments of this nature should include various thicknesses of target materials, as well as regulation of the laser output energy and the pump lamp pulse length. The laser beam intensity per unit area should be adequate to melt only the target surface, and in other cases adequate to vaporize the surface. Laser spot defocusing can also be used as another variable parameter.

Acknowledgments

I would like to express my appreciation to Mr. Frank Dawson of the Components Division for his able assistance in setting up and operating the camera, and to Mr. William J. Robinson for his assistance in setting up the experiment.

References and footnotes

1. J. F. Ready, *J. Opt. Soc. Am.* **53**, 514 (April 1963); abstract only.
2. J. F. Ready, *Applied Phys. Letters* **3**, 11 (1963).
3. D. Lichtman and J. F. Ready, *Phys. Rev. Letters* **10**, 342 (1963).
4. G. A. Askar'yan and E. M. Moroz, *Soviet Phys. (JETP)* **13**, 1638 (1963).
5. R. E. Honig, *Applied Phys. Letters* **3**, 8 (1963).
6. F. Giori, L. A. MacKenzie and E. J. McKinney, *Applied Phys. Letters* **3**, 25 (1963).
7. R. E. Honig and J. R. Woolston, *Applied Phys. Letters* **2**, 138 (1963).

Received July 31, 1963